Journal of
Manufacturing and Materials Processing

MDPI

Review

Linking Process Parameters, Structure, and Properties in Material Extrusion Additive Manufacturing of Polymers and Composites: A Review

Attila Debreceni [1,2,*], Zsolt Buri [3,4] and Sándor Bodzás [1,5]

1 Department of Mechanical Engineering, Faculty of Engineering, University of Debrecen, 4028 Debrecen, Hungary
2 Doctoral School of Informatics, University of Debrecen, 4028 Debrecen, Hungary
3 Department of Engineering Management and Enterprise, Faculty of Engineering, University of Debrecen, 4028 Debrecen, Hungary
4 Doctoral School of Management and Business, University of Debrecen, 4032 Debrecen, Hungary
5 Pekar Imre Doctoral School of Mechanical Engineering, University of Debrecen, 4028 Debrecen, Hungary
* Correspondence: debreceni.attila@eng.unideb.hu; Tel.: +36-307170455

Abstract

This review investigates how process parameters and material choices influence the mechanical performance of parts produced by material extrusion additive manufacturing, with a particular focus on Material Extrusion (ME). Through a systematic bibliometric analysis of literature between 2015 and 2025, the study identifies key factors affecting mechanical strength, anisotropy, and structural reliability, including printing temperature, speed, orientation, layer thickness, and interlayer bonding. Emphasis is placed on emerging techniques such as 4D printing, fiber-reinforced composites, and novel monitoring methods like real-time vibration sensing and thermal imaging, which offer promising pathways to improve part performance and process stability. Three research questions guide the analysis: (1) how printing parameters affect micro- to macrostructure and failure behavior, (2) how optimization strategies enhance part quality, and (3) how material and process selection aligns with functional requirements. The review highlights both advances and persistent limitations in process control, material compatibility, and anisotropic strength. It concludes with a call for further integration of predictive modeling, hybrid material systems, and closed-loop process monitoring to unlock the full potential of additive manufacturing in high-performance engineering applications.

Keywords: additive manufacturing; bibliometric review; mechanical properties; microstructure; mesostructured; macrostructure; fused deposition modeling; fused filament fabrication

check for updates

Academic Editors: David L. Sales, Severo Raul Fernandez-Vidal and Tiago Vieira Da Cunha

Received: 11 July 2025
Revised: 12 August 2025
Accepted: 16 August 2025
Published: 22 August 2025

Citation: Debreceni, A.; Buri, Z.; Bodzás, S. Linking Process Parameters, Structure, and Properties in Material Extrusion Additive Manufacturing of Polymers and Composites: A Review. *J. Manuf. Mater. Process.* **2025**, *9*, 286. https://doi.org/10.3390/jmmp9090286

1. Introduction

1.1. Challenges in Additive Manufacturing

Additive manufacturing (AM) has been introduced as a relatively recent production method, with the first commercial technology appearing in the late 1980s [1]. The earliest AM process was stereolithography (SL/SLA), in which a UV laser was used to solidify photopolymer resins layer by layer, facilitated by a platform that moved downward into the resin [2–4]. A related method, digital light processing (DLP), differs in that it uses a light source that illuminates an entire layer at once, resulting in faster production [2]. In 1991, three additional AM techniques were developed: fused deposition modeling (FDM also called Fused Filament Fabrication or FFF), solid ground curing (SGC), and laminated object manufacturing (LOM) [1]. Among these, FDM became the most widely adopted. In FDM, thermoplastic filament is fed into a heated extruder, melted, and deposited layer by layer onto a heated build plate [2–4]. Since FDM and FFF generally describe the same process (and different sources may use one term or the other), they are referred to as material extrusion (ME) in this text for clarity. In 1992, selective laser sintering (SLS) was introduced [1], which utilizes a high-power laser to sinter powdered material layer by layer. A roller is used to distribute powder from a feed chamber to a build chamber in a uniform layer, allowing both metallic and non-metallic materials to be processed [2–4].

High-quality prints in terms of mechanical properties, surface finish, and geometry are achieved through the selection of appropriate materials and process parameters. The attainment of the desired quality is generally regarded as a process parameter optimization problem [5]. Many everyday faults in ME are attributed to incorrect machine calibration, unsuitable process parameters, or inappropriate material selection [6].

Process parameters such as part orientation, layer thickness, printing speed, part size, and support design are recognized as significantly influencing accuracy, productivity, cost, and material usage [7]. Reduced tensile strength and anisotropy are caused by poor interlayer bonding or high void content, whereas stiffness and durability are improved under optimal thermal conditions [8]. Considering these relationships, a bibliometric review of ME additive manufacturing was conducted. Research results from 2015 to 2025 were mapped to assess advancements in achieving high-quality prints. The following research questions were used to guide this review:

- Question 1 (RQ1): How do printing process parameters influence the micro-, meso-, and macrostructure of various commonly used polymer materials, as well as their mechanical properties and failure modes?
- Question 2 (RQ2): How can various factors, like the printing process and post processing, be optimized to improve crucial structural and mechanical properties, as well as the quality of the prints?
- Question 3 (RQ3): How can the desired properties of printed parts be used to choose the ideal material and printing parameters.

1.2. Common Materials in Reviewed Articles

In additive manufacturing, a range of materials, including metals, plastics, ceramics, and composites, are used [6,9–11]. However, due to the prevalence of polymer-based technologies, this article focuses on polymer materials, specifically in the context of ME.

Polymers, also known as plastics, are synthetic, semi-synthetic, or natural macromolecular materials that are characterized by diverse physical and mechanical properties [12]. These materials are composed of small molecules called monomers, which can be bonded together under ideal conditions, which is known as polymerization [13]. Polymers are generally classified into two categories: thermoplastics and thermosets [14,15]. Thermoplastics can be melted many times and solidified upon heating and cooling, without significant degradation of their properties. In contrast, thermosetting plastics undergo a one-time reaction and cannot be remelted once set without degradation, limiting their recyclability. The selection of manufacturing technologies such as injection molding, extrusion, or thermoforming is largely influenced by whether a polymer is thermoplastic or thermosetting.

The most common ME materials in the reviewed papers were PLA, ABS, and PA, which were sometimes used as matrices in composites. PLA is favored for its low cost, ease of processing (due to its low print temperature and minimal warping), and biodegradability [16]. However, its mechanical properties are weak, limiting its use in technical applications [11,17]. PLA is also valued for its biocompatibility, and when it is used as a matrix in composites, enhanced mechanical performance can be achieved [18]. For instance, a study by Li et al. [19] demonstrated that flexural strength could be significantly improved through treatment in dichloromethane. Still, the relatively low tensile strength remains a limitation; Tymrak et al. [20] reported a value of approximately 62 MPa under optimal conditions. Overall, PLA is a low-cost, user-friendly material, though limited by its mechanical strength and toughness [11,21]. ABS is another commonly used material in AM and had already been widely employed before the advent of 3D printing [11,22]. Its popularity is attributed to its availability, impact resistance, and thermal stability. However, ABS tends to warp under thermal stress, leading to delamination and detachment from the build plate unless a heated chamber is used, which is something not available in basic consumer printers [11,14,21–23]. According to Ning et al., unreinforced ABS exhibited a tensile strength of 34 MPa and 4% elongation at break [24]. PA, particularly PA 6 or PA 6 and PA 12 or PA 12 variants, is also frequently used in ME printing [25]. PA 6 offers high strength, abrasion resistance, and thermal stability but is highly hygroscopic and prone to warping, making it difficult to print [11,26]. Conversely, PA 12 absorbs less moisture, warps less, is easier to print, and shows greater chemical and UV resistance, though it has slightly lower mechanical and thermal properties. PA 6 is typically used for high-stress, heat-resistant parts, while PA 12 is more suitable for applications requiring long-term stability under adverse conditions [11,25].

2. Materials and Methods

Used Methodology

During the review, various methods were employed to understand the current state of research on the mechanical properties of 3D-printed materials. In this chapter, the chosen methods and scores will be introduced.

The Global Citation Score (CCS) was utilized as a score to find relevant, widely accepted articles in general. It is the total citation count of the article, while Local Citation Score normalizes it by only including the citation count from a specific field [27]. This paper will use the GCS normalized by year metric to ensure that older articles are not over-represented.

Co-citation is a method from the 1970s that is an effective way to map the field of research; it identifies which documents are usually cited together by other researchers [28]. Co-citation is important because it enables the identification of similar works in a specific research field, facilitating the identification of influential papers, research trends, and new areas of study [29,30]. VOSviewer 1.6.20 is a software platform that can be used to visualize bibliometric networks. Relationships between co-cited authors, papers, or journals are identified, and clusters can be created to visualize them. The articles are highlighted by the software, which enables the quick identification of important papers in a specific field [31,32].

The event known as a "burst of activity" describes the increase in popularity of a paper, author, or keyword over a period [33]. Such bursts reflect emerging trends and increase scholarly attention within a specific research field. Burst detection is particularly valuable in bibliometric analysis, as it helps identify and predict popular research topics [34]. A keyword with a strong citation burst means an increase in research in a specific field or a growing consensus on a novel approach or topic. Similarly, burst activity of a publication can indicate important findings in a specific field, or it can be a node between many fields. CiteSpace can be used to generate various scientific visualizations, including burst timelines of keywords or articles based on a Scopus index export [35,36].

Co-occurrence network analysis of keywords is used to explore the structural patterns and emerging trends within a research field. By analyzing the frequency with which keywords appear together in scholarly articles, this method reveals thematic relationships and highlights connections between different areas of research [37]. VOSviewer can be employed to visualize and identify clusters of related keywords. By exporting the map file, the occurrence of all keywords can also be quantified numerically [38].

In Figure 1, the structure of the bibliometric analysis of this article is shown. The first significant step was to create a comprehensive dataset of articles to answer the research question. The basis articles of the systematic literature review were found on Scopus. Scopus was launched in 2004 by Elsevier [39], and it has become one of the most popular scientific databases, containing more 2.5 million independent article indexes in 2020 [40,41].

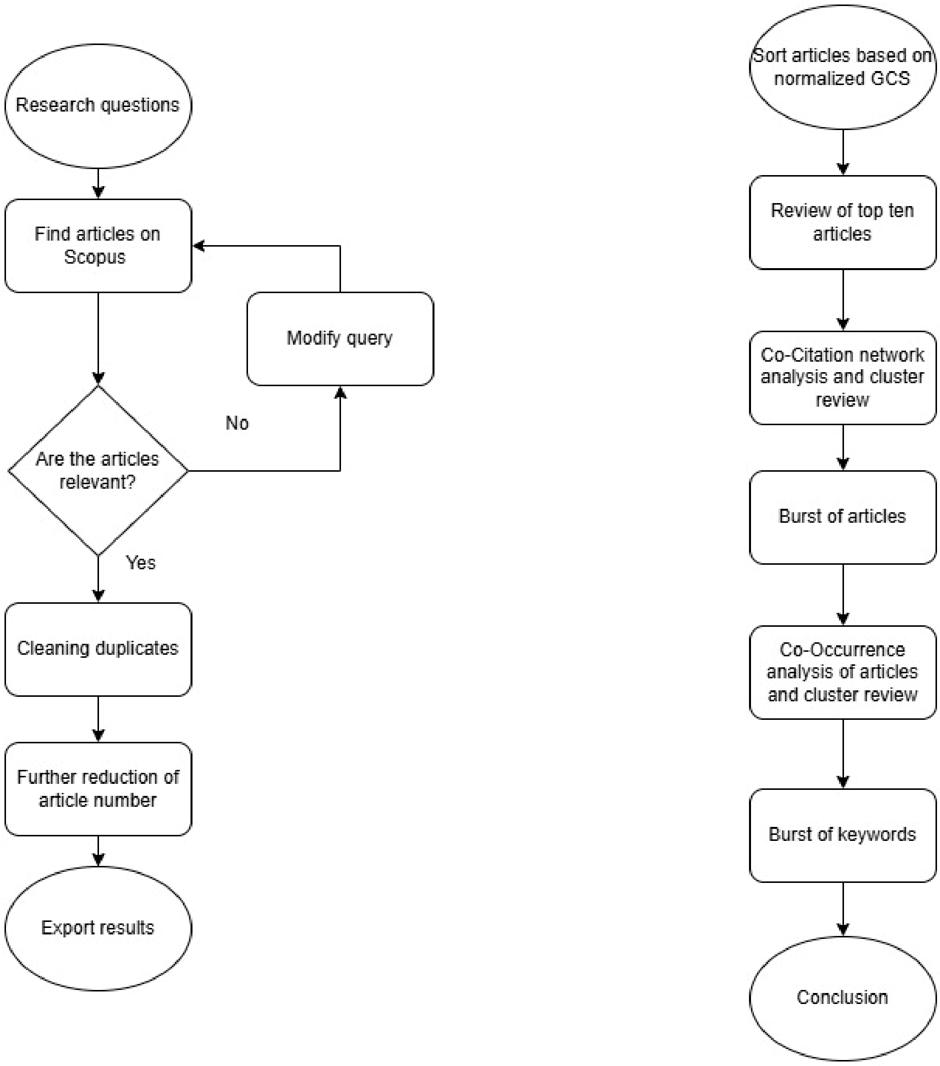

Figure 1. Flowchart of the bibliometric review.

First, the following query was utilized in advanced search mode to find relevant articles:

Additive manufacturing AND (ME OR fff OR material extrusion) AND printing AND parameters AND mechanical properties AND NOT medical AND NOT metal AND NOT construction AND NOT concrete AND NOT food.

The AND NOT operators were required to filter out articles that were not relevant for the scope of this review. Only articles published within a 10-year interval (2015–2025) were examined. After this, duplicated datapoints were removed, and the number of articles was further reduced. For this, additional filters were applied; for example, language filters were applied, the article type was set to journal article, and relevant subject areas were selected.

3. Results

This chapter presents the methods applied in the study and the obtained results. In Section 3.1, the top 10 articles based on their normalized GCS are examined. In Section 3.2, a co-coupling network is created via VOSViewer. The four most important articles from each cluster were further examined.

3.1. Important Articles Based on GCS

Heidari-Rarani et al. [42] developed a new extruder to enable continuous CF PLA part production on an already existing machine. They also implemented surface preparation via PVA. Experimental results show tensile and bending strength increases of up to 35% and 108%, respectively, compared to pure PLA. They also identified matrix cracking as the most important failure mode [42]. Senatov et al. [43] developed porous scaffolds from PLA with 15 wt% hydroxyapatite (HA). HA-improved rigidity caused a shape memory effect at 70 °C and, overall, provided a self-healing property to the material, but the high temperature probably does not support any biological application. ABS incorporated with 4 wt% xGnP was experimented on by Dul et al. [44]. The elastic and storage moduli, as well as the thermal stability, were enhanced by xGnP, while the ultimate tensile strength decreased. Various printing orientations were also examined, with a horizontal build orientation found to perform the best.

Wang et al. [45] used short CF- and short GF-reinforced PEEK composites from 5 to 10 wt%. The reinforcements were found to increase thermal stability and mechanical properties. GF was bonded better than CF with the matrix, which was caused by effective surface treatment. Microstructural analyses were conducted, showing that fiber alignment in the print direction increases mechanical performance. Magneto-responsive SMP filaments from PLA, TPU, and Fe_3O_4 were developed by Liu et al. (4D printing) [46]. A 99% shape fix and a 96% recovery ratio were measured, while the tensile strength (54 MPa) and Young's modulus (1200 MPa) were conserved. The effect of microscopic voids (the absence of matrix material) between continuous fiber reinforcement was investigated by He et al. [47]. A void volume of 12% was observed in the CF PA6 composite. These voids were identified as the main factor contributing to reduced mechanical performance. By decreasing the void content, a 93% improvement in mechanical performance was observed.

The BAAM system, developed by Oak Ridge National Laboratory, was investigated by Duty et al. [48]. This system utilizes large-scale 3D printing technology, where pellet-fed thermoplastics are used instead of filament. It was demonstrated that this method is 20 times cheaper and 200 times faster than traditional ME. Parts up to 6 m × 2.4 m × 1.8 m can be printed, and the system performs well with fiber-reinforced composites, improving stiffness but increasing anisotropy and porosity. The effect of extrusion and printing speed on the dimensional accuracy and microstructure of PEEK filament was investigated by Geng et al. [49]. Extrusion force and melt pressure were identified as the main factors affecting accuracy. A control algorithm was developed to increase surface quality by mathematically replacing the nozzle diameter with the diameter of the extruded filament and extrusion speed. Effects of nozzle temperature, build-stage temperature, and printing speed on the interfacial bonding of TPU/ABS in multi-material ME were examined by Yin et al. [50]. Bonding strength increased by 93% when the build-stage temperature was raised from 30 °C to 68 °C. Bonding behavior was accurately predicted by a heat transfer-based diffusion model, which showed strong correlation with experimental results. These findings support better process control to enhance mechanical performance in multi-material ME. A continuous flax fiber-reinforced PLA composite was studied by Duigou et al. [51] using a newly developed co-extrusion process applied to a Prusa i3. A tensile strength 4.5 times higher and stiffness 7 times greater than those of pure PLA were achieved by the composite.

These results were found to be comparable to those of continuous GF PLA composites while offering the advantages of being a biocomposite.

3.2. Co-Coupling Network

Figure 2 shows the co-coupling network of the Scopus dataset. Five clusters can be observed; *Cluster 1* is red, *Cluster 2* is green, *Cluster 3* is blue, *Cluster 4* is yellow, and *Cluster 5* is purple. The minimum number of citations was set to 100. The association strength method was used for link strength normalization [52]:

$$S_A\left(c_{ij}s_is_j\right) = \frac{c_{ij}}{s_is_j} \quad (1)$$

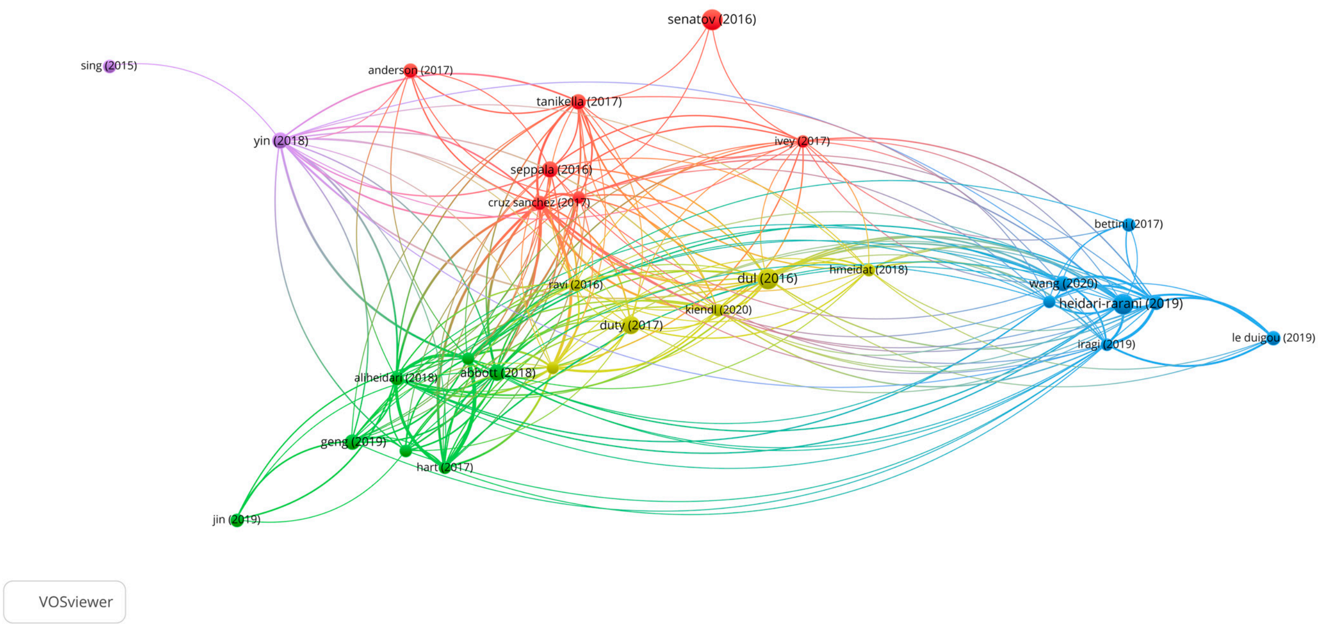

Figure 2. Co-coupling network created with VOSViewer.

In Cluster 1 (red), the mechanical behaviors of parts made from PLA are presented. Research by Anderson et al. [53] and Cruz et al. [54] focused on recycled material. Significant decreases in yield, ultimate, and break tensile strength were observed. In addition, shear yield strength increased by 6%, while Shore hardness decreased by 2.5%. The effect of seven printing parameters on mechanical behavior was investigated by Hikmat et al. [55], with build orientation, infill density, and nozzle diameter identified as statistically significant factors. The effect of printing parameters on short CF PLA was investigated by Ivey et al. [56]. They found that the addition of short CF significantly increased the elastic modulus but also caused the formation of voids in the material. Heat treatment was shown to improve the crystalline structure. Overall, the common focus in this cluster is sustainability (biodegradable materials) and advanced research into mechanical properties.

The articles in Cluster 2 (green) present research on various materials. A strong emphasis is placed on the effects of interlayer bonding, thermal conditions, and the use of imaging techniques. Weak bonding between PLA and lignin was reported by Gkartzou et al. [57], resulting in brittleness and failure. Scanning electron microscopy was utilized in the study, revealing that a rougher PLA/lignin surface increased adhesion but also resulted in a higher volume percentage of voids. In the case of ABS, interlayer bonding was found by Abbott et al. [58] to be closely linked to thermal history and interfacial contact. Geng et al. [49] reported that melt pressure and extrusion force significantly influence the interlayer bonding and dimensional accuracy of PEEK-based prints. The mechanical behavior of ABS-based parts was studied by Aliheidari et al. [59], with a focus on fracture resistance. Nozzle temperature, bed temperature, layer height, interlayer bonding, and mesostructure were found to have significant effects on fracture behavior. Overall, the common theme among these articles is the influence of the thermal characteristics of the printing process, either directly on mechanical properties or indirectly through their impact on interlayer bonding and microstructure.

Cluster 3 (blue) contains articles related to continuous fiber-reinforced printing. The works of He et al. [47] and Heidari-Rarani et al. [42] have already been discussed in Section 3.1. The flexural properties of continuous CF PLA composites were investigated by Hu et al. [60], and a quadratic regression model was fitted to the resulting dataset. The model's weight coefficients indicated that layer thickness was the most significant factor, followed by printing temperature and printing speed. Aramid fiber reinforcement with PLA as the matrix was used by Bettini et al. [61]. This composite was shown to perform significantly better than plain PLA, with increases observed in both ultimate tensile strength and ultimate compressive strength.

Cluster 4 (yellow) contains articles that used various material extrusion-based technologies and subject materials. Dul et al. [44] used graphene nanoplatelets with ME, and Duty et al. [48] investigated the BAAM method with fiber-reinforced thermoplastics as material. Alaimo et al. [62] investigated the effect of chemical composition and the inner mesostructure of ABS filament on mechanical properties. The research concluded that macromechanical properties can be significantly influenced by the chemical composition and mesostructure of ABS. Increasing the filament cross-section generally leads to higher stiffness and shear modulus and lower tensile strength and strain at 0° fiber orientation but higher tensile strength and strain at 90°. Hmeidat et al. [63] introduced an epoxy/clay mixture as material for DIW. Flexural modulus and strength increase with clay content, with printed longitudinal specimens showing higher values due to anisotropic alignment of fillers during printing. Strain to failure ranges from 3 to 5%, with longitudinal samples consistently outperforming transverse ones, suggesting that flaws between filaments reduce transverse performance. These studies focused on the micro- and mesostructure of materials, emphasizing the importance of anisotropy based on filler and print orientation.

3.3. Burst of Articles

Many articles have shown a high burst of activity in recent years. The six articles shown in Figure 3 with high burst activity will be reviewed in this subchapter.

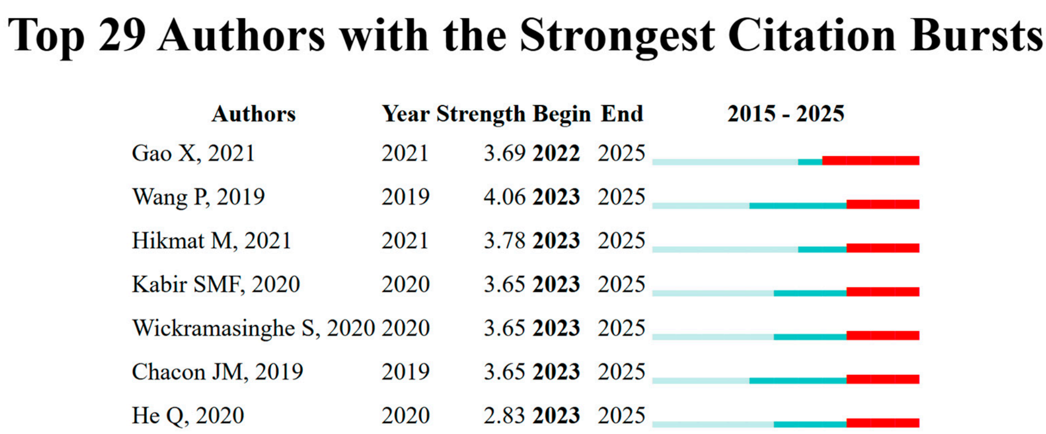

Figure 3. Articles with high bursts of activity in recent years [50,64–68]. The red bar is used to highlight the burst duration, the turquoise bar to represent the publication years of the article, and the light-blue bar to indicate the years before its publication.

Gao et al. [64] reviewed the bonding mechanisms between layers in ME printed parts. In amorphous polymers, interlayer bonding was described as occurring through viscous sintering and molecular diffusion; however, rapid cooling was found to limit the effectiveness of interdiffusion. Chain entanglement recovery was also identified as a dominant factor. For semicrystalline materials, stronger bonding can be achieved, particularly when partial remelting and chain relaxation are applied. The variations in interlayer bonding strength can be understood through polymer chain diffusion and viscous sintering models, which explain how cooling rates and layer interface conditions affect bonding efficiency. It was concluded that ABS and PLA exhibit mechanical anisotropy of approximately 50%, while PEEK and TPU show around 20% and PP and PA exhibit even lower levels. The observed anisotropy was attributed to factors such as build orientation, raster angle, and whether the material is fiber-reinforced.

The mechanical properties, surface quality, and microstructure of PEEK were investigated by Wang et al. [65] in relation to various printing parameters. Finite element analysis was utilized to examine the fluidity and melting conditions of PEEK to determine the optimal printing parameters. Using a printing temperature of 440 °C, a layer thickness of 0.1 mm, and a printing speed of 20 mm/s, 80% of the tensile strength of injection-molded PEEK was achieved through ME. However, increased brittleness was observed compared to the injection molding method. SEM images confirmed the presence of more brittle fracture surfaces in the ME-printed parts compared to those produced by injection molding. Finite element thermal models can also reveal how temperature gradients during printing influence crystallinity and bonding, thereby affecting mechanical performance.

A comprehensive review on continuous fiber-reinforced 3D printing was published by Kabir et al. [66]. The review covered fiber–matrix bonding; void formation; microstructural failure modes; and various mechanical properties, including tensile, flexural, compression, shear, and impact strength, as well as critical process parameters. Delamination and void formation were identified as the main limitations of ME technology. Delamination was noted to prevent the formation of a true three-dimensional connection between composite layers, while voids between the matrix and fiber, as well as between layers, were found to significantly reduce the strength of the printed parts. Most ME systems are not capable of producing hybrid composites without manually stopping the printer, which reduces overall productivity. Additionally, commercial printers typically do not permit the adjustment of many key parameters.

In addition to discussing the limitations of ME technology, Kabir et al. reviewed various predictive models used to simulate and analyze the mechanical and structural behavior of continuous fiber-reinforced composites produced by ME [66]. These models include Finite Element Analysis (FEA), Volume Averaging Stiffness (VAS), Rule of Mixing (ROM), and the Park and Rodriguez models, as well as damage initiation theories like Hashin's model. FEA was highlighted for its ability to predict failure modes and optimize mechanical properties by considering fiber orientation, fiber volume fraction (FVF), and infill patterns. While ROM provides reasonable tensile property estimates at low fiber contents, VAS is preferred for higher fiber fractions due to its micromechanical basis. The review emphasized that these predictive approaches are valuable tools for understanding composite performance and guiding design improvements, although further research is needed to address anisotropic and inhomogeneous behaviors unique to 3D-printed composites.

ME polymers and composites were reviewed by Wickramasinghe et al. [67]. It was found that ABS, PA, and PLA are the most widely used materials. Based on the reviewed literature, a 10% fiber volume fraction (FVF) of short fiber reinforcement (SFR) was generally identified as optimal. Fracture surface analysis revealed that failure can occur due to fiber pull-out, fiber breakage, and debonding. These failure modes can be mitigated through chemical or thermal treatments. Printing in a vacuum or nitrogen atmosphere was reported to improve surface quality. Additionally, ultrasound was identified as a versatile technique for enhancing multiple characteristics of printed parts by improving fiber–matrix bonding, reducing the staircase effect, enhancing surface quality, and decreasing void volume.

The mechanical performance of ME-printed PA composites reinforced with continuous carbon, glass, and Kevlar fibers was studied by Chacón et al. [68]. Tensile and flexural tests revealed that a flat build orientation significantly enhanced strength and stiffness compared to an on-edge orientation. The best mechanical performance was achieved with carbon fiber reinforcement, while Kevlar exhibited the weakest results due to its poor compressive resistance. Fiber pull-out was observed, indicating weak fiber–matrix bonding, which was attributed to inadequate fiber coating. Although higher fiber content led to improved strength, the gains plateaued due to void formation and insufficient interlayer adhesion. To address these issues, a post-deposition compaction stage was recommended to deal with porosity and improve overall mechanical performance.

3.4. Keyword Co-Occurrence Network and Burst Analysis

The most frequently co-occurring keywords were examined. A co-occurrence network was generated using VOSviewer to identify the strongest keywords. The generated network presented is in Figure 4. A minimum keyword occurrence threshold of 50 was applied, and the minimum line strength was set to 20 to eliminate connections between weakly linked keywords, thereby enhancing visibility.

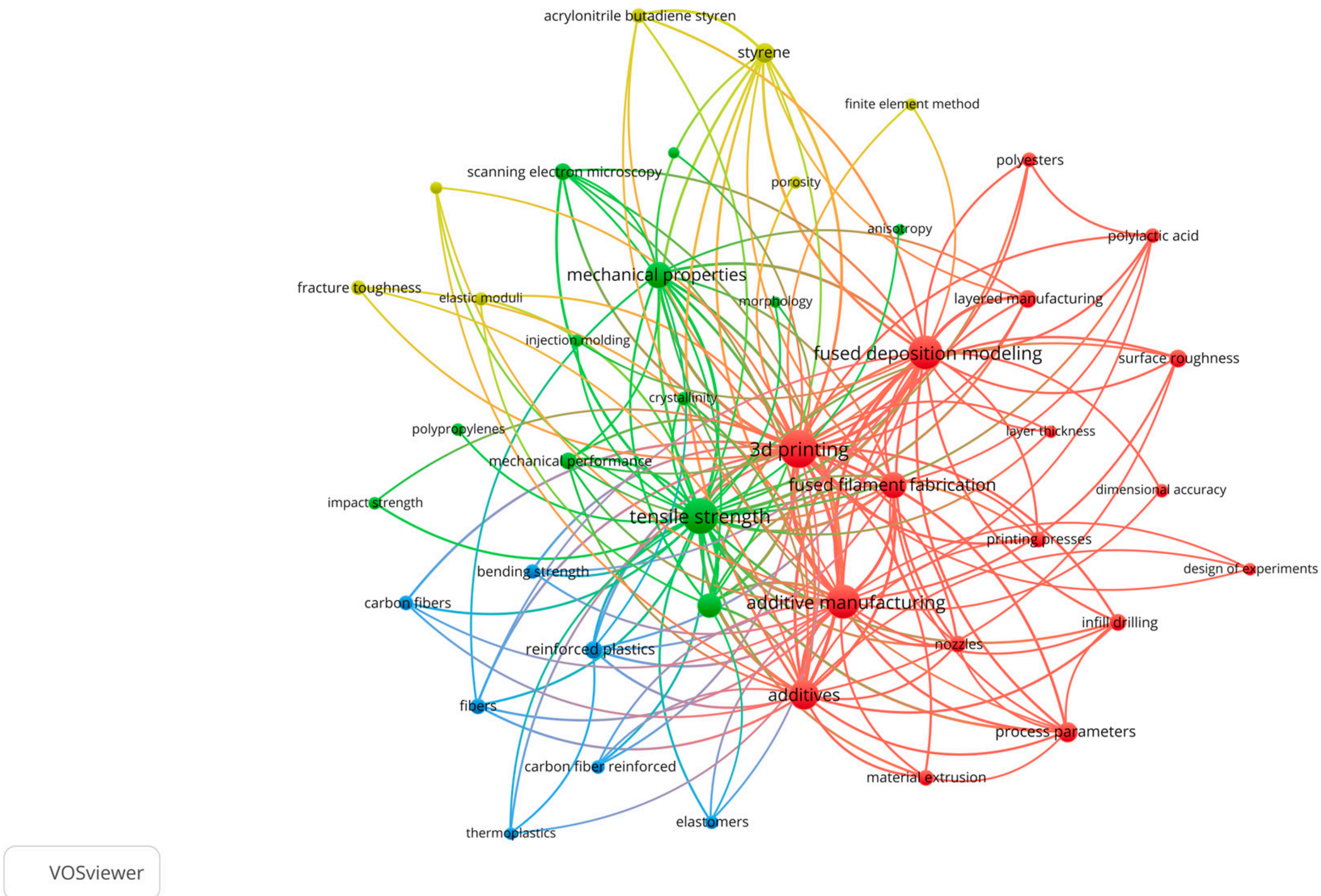

Figure 4. Co-occurrence network of keywords.

After the four most prominent keywords were identified, the most relevant articles were selected based on a Scopus search using the predefined query. The four most cited papers containing the cluster keywords were then reviewed. In cases where one or more of the four most cited papers had already been reviewed, the following most cited articles were considered. As the terms 3D printing, additive manufacturing, mechanical properties, and ME were already included in the initial query, the next most frequently used keywords were employed to identify additional relevant articles.

Cluster 1 (red) contains keywords related to manufacturing technologies and print quality. The influence of the raster layup on the mechanical properties (toughness, strength, and stiffness) of ME 3D-printed PLA parts was investigated by Kiendl et al. [69]. It was found that unidirectional raster layups show the highest strength and stiffness when they are aligned with the loading direction. However, toughness was low due to brittle fracture. In standard alternating layups, stiffness and strength were found to be nearly isotropic, while toughness showed significant anisotropy. Ductile behavior was observed when loading was applied diagonally to the raster. A new layup scheme was proposed to optimize both strength and toughness, achieving up to a 17% increase in strength and a 462% increase in toughness compared to unidirectional layups. Future work was proposed to extend these findings to multiaxial loading scenarios and to develop advanced numerical models capable of capturing mesoscale effects.

A system was developed by Jin et al. [70] that utilizes computer vision and deep learning to detect and correct common 3D printing issues in real time. A camera was mounted near the printer nozzle to record images of the printed part, which were used by a convolutional neural network (CNN) trained to classify print quality into categories such as “good”, “under-extrusion”, and “over-extrusion”. The system was designed to adjust the printer’s flow rate automatically to correct detected issues. The CNN model, based on ResNet-50, achieved an accuracy of 98% in identifying print defects. Detected problems could be corrected within seconds. The authors suggested that this approach could be extended to other 3D printing technologies and more complex categories of defects in future research.

A system was developed by Ravi et al. [71] to improve the strength of ME 3D-printed parts with a near-infrared laser for the preheating of already printed layers before deposition. To better understand the thermal effects of localized laser preheating during the build process, a transient heat-transfer finite element model was constructed using COMSOL. This model simulates the laser as a traveling Gaussian heat source on the polymer surface, incorporating experimentally measured optical and thermal properties of ABS. The resulting temperature profiles provide insight into the temperature gradients and interface temperatures critical for polymer chain diffusion and interlayer bonding strength. These modeling results correlate well with the observed mechanical improvements and microstructural changes in laser-heated samples. Interlayer bonding was improved by up to 50% due to laser preheating, resulting in a change in fracture behavior from brittle to ductile. Enhanced polymer chain diffusion was achieved, particularly strengthening the parts in the build direction. However, it was observed that excessive laser power introduced defects. The method was demonstrated to be promising for the production of stronger and more reliable components, with future research focusing on optimizing the laser parameters for broader applications.

Tlegenov et al. [72] presents a vibration-based nozzle condition monitoring technique for ME 3D printers, addressing the common issue of nozzle clogging that degrades part quality. By modeling the extruder’s bar mount as a pinned–pinned beam and analyzing its vibrations using a MEMS accelerometer, the researchers demonstrated that clogging causes a measurable and non-linear increase in vibration amplitude. Experiments conducted on

PLA, ABS, and SemiFlex filaments using both direct and Bowden extruders confirmed the theoretical predictions, with close alignment in natural frequency and amplitude data. A custom 3D printer with a fixed extruder was built to minimize external disturbances, and the sensor setup proved to be both accurate and cost-effective. Despite minor discrepancies due to unmodeled factors such as filament radius variation and sensor mass, the method demonstrates strong potential for real-time, low-cost clog detection and lays the groundwork for more reliable ME printing.

Cluster 2 (green) contains keywords related to materials science, polymers, and micro- and mesostructure. Some articles related to this cluster have already been discussed. To further expand this field, four additional articles were reviewed.

Research on printable materials using different material extrusion processes (ME, BAAM, and DIW) was conducted by Duty et al. [73], who developed a "Printability Model". This model predicts whether a specific material can be printed based on defined "fail/pass" conditions such as nozzle flow, fiber clogging, geometry creation, and geometry stability. Bounding equations were used as printing criteria that must be satisfied to meet these conditions and pass the test. For instance, the nozzle flow criterion is based on the Hagen–Poiseuille equation, adapted to account for non-Newtonian fluid behavior typical of printing materials. This equation helps predict whether the material can be extruded steadily without clogging or excessive pressure buildup. The model also includes a fiber clogging criterion, which assesses the risk of blockage during extrusion, and geometric stability equations that determine if the printed shape can maintain its form during and after printing without collapsing. While the authors noted that the system can be improved, the current results demonstrate that the model is already practical for use.

The effect of process parameters on the inter- and intralayer strength of PLA was investigated by Spoerk et al. [74], with the goal of improving bonding between layers. Tensile and double-cantilever beam tests were conducted, and statistical methods were utilized for evaluation alongside optical microscopy images. Printing temperature, layer thickness, and shifted layer design, which have already been proposed as factors for improving surface quality, were examined. Statistical evaluation of the tensile tests indicated that layer height was the most significant factor, while layer design was more important than temperature, as tensile strength was found to be nearly independent of temperature. Similar results were obtained from the double-cantilever beam tests. A printing temperature of 250 °C and a layer thickness of 0.25 mm were identified as preferable for improved bonding between strands.

Tanikella et al. [75] studied the tensile properties of printed parts with various materials with different color agents (ABS, HIPS, PC, PA618, TPU, etc.). The test species were printed with 100% infill density in a temperature-controlled environment. The printing temperatures varied based on which material was used. The crystallinity of PLA can vary based on its color due to the coloring agents noted in a previous paper [76]. The mass of the printed part showed a strong correlation with its mass (except PA 618). The authors mentioned limitations of this research. The study acknowledges limitations in measuring filament density per color (rather than per material group), which could affect mass comparisons, mainly since densities similar to that of water introduce measurement sensitivity. Additionally, crosshead extension focused only on the specimen's reduced section, impacting strain calculations but not maximum stress values.

Wittbrodt et al. [77] studied the mechanical properties of PLA parts printed by ME, focusing on the effects of printing temperature and post-print thermal annealing. The specimens were printed at nozzle temperatures ranging from 195 to 255 °C, then annealed at temperatures between 65 and 95 °C, above the glass transition temperature. Crystallinity was measured using differential scanning calorimetry (DSC) and X-ray diffraction (XRD), while mechanical performance was evaluated through three-point bending and tensile tests. The results showed that annealing increased crystallinity by up to 25% and improved flexural stress by 11–17%. However, radiation sterilization caused a reduction in molecular weight and mechanical strength by 20–30%. The authors noted challenges in balancing processing temperatures to prevent PLA degradation and ensuring even heat distribution during the annealing process.

Cluster 3 (blue) centers on advanced material keywords, with a particular focus on fiber-reinforced plastics that enhance tensile and flexural strength. Dou et al. [78] investigated the tensile properties of continuous CF PLA using various printing parameters on a modified RepRap Kossel printer. A one-factor-at-a-time (OFAT) design of experiments (DoE) was used. They found that layer height and extrusion width had the greatest influence on tensile strength and stiffness, primarily due to their effect on relative fiber content. In contrast, printing temperature and speed mainly affected the fiber–matrix interface, with comparatively lesser impact on mechanical properties. The study identified poor bonding at the fiber–matrix interface, often leading to fiber pull-out, as the dominant failure mode. However, the authors did not account for parameter interactions due to the limitations of the OFAT approach, nor did they explore alternate fiber placement strategies or optimization techniques. Future research could benefit from factorial or response surface methodology (RSM) designs to better capture variable interdependencies.

Iragi et al. [79] studied the intra- and interlayer behavior of a continuous CF PA6 composite using a Markforged MarkTwo printer. They determined ply-level elastic and strength properties and analyzed production defects. Void content was confirmed to be higher in the printed parts than in the original filament. The composite exhibited high longitudinal strength, with brittle fractures mostly occurring between beads and layers, indicating strong fiber–matrix bonding. However, transverse tension performance was weak and brittle, while compression tests showed more ductile behavior. In-plane shear failures involved fiber breakage and interlayer delamination. Interlaminar fracture tests revealed stable crack growth, with fiber bridging improving mode I toughness, though mode II toughness was lower—likely due to structural characteristics. These results underscore the role of bead arrangement and interlayer bonding in the anisotropic nature of ME parts, where strength is greatest along the filament direction. The study's limitation lies in its focus on unidirectional laminates and standardized testing, which may not reflect the complexity of real-world applications.

Calignano et al. [80] conducted research similar to that Iragi et al. [79]. Both studies demonstrate that build orientation and infill percentage significantly influence mechanical properties in carbon fiber-reinforced prints. While both find that an XZ orientation results in stiffer but more brittle parts and an XY orientation yields tougher, more resilient components, Calignano's work uniquely highlights that 80% infill may offer better energy absorption than 100% infill, likely due to reduced thermal stresses and improved interlayer adhesion.

Reich et al. [81] examined the mechanical performance of recycled polycarbonate (PC) using tensile and compression tests, printed with the Gigabot X, a fused granular fabrication (FGF) machine. A speed–temperature matrix was developed to minimize the deviation between theoretical and actual extruded mass. Using the optimal parameters, a 12.5× higher deposition rate was achieved compared to traditional ME printers. While the Gigabot X achieved a UTS of 64.9 MPa, slightly outperforming the 62.2 MPa reached by a standard TAZ6 ME printer, compression strength was significantly lower. In some cases, compressive stress in Gigabot X prints reached only 56% of that achieved by TAZ6. The study concludes that FGF cannot fully replace ME when fine resolution and high compressive performance are required, mainly due to limitations in nozzle size and layer control.

The keywords in *Cluster 4* (yellow) are mostly related to mechanical properties, finite element analysis, and ABS.

Bodaghi et al. [82] developed an ME 4D printing method of planar adaptive SEM materials that can self-transform after fabrication. In the printing process, this self-transforming effect was programmed into the printed parts by adjusting the ME printer nozzle temperature and printing speed, which influenced the amount of residual stress stored and the degree to which the polymer chains were stretched and relaxed. FEA was utilized to predict and validate the method. Using FEA, they were able to express the printing parameters numerically and link to residual stresses. Equations were derived based on the non-linear Green–Lagrange strains. They were then solved by an iterative incremental Newton–Raphson scheme to trace the non-linear equilibrium path in the large-deformation regime. Additional modeling incorporated temperature-dependent material properties into the constitutive framework, enabling more accurate prediction of transformation onset and recovery forces. The simulation outputs were validated against experimental deformation profiles, showing strong agreement in both curvature evolution and final shape recovery. The authors discussed the possible applications; this method enables minimally invasive delivery of medical devices in compact, temporary shapes that expand or tighten when exposed to body temperature. This allows for tailored, patient-specific treatments with reduced surgical complexity and faster deployment. However, limitations include issues with respect to precise control of transformation behavior, sensitivity to temperature variations, and long-term material stability in biological environments.

Davis et al. [83] studied the strength of ME-printed ABS part welds (layer adhesion/bonding) by measuring fracture strength. They identified that the weld thickness is largely independent of print velocity, significantly correlated with the printing temperature. The weld strength is dependent on the nozzle temperature and, to some extent, on the printing speed. It is important to note that the temperature still has a greater effect on the strength, increasing by around three times, while speed only has a minimal impact.

Hart and Wetzel [84] investigated how layer orientation affects the fracture behavior of 3D-printed ABS materials using single-edge notch bend (SENB) testing. They found that cracks propagating between layers (interlayer) require significantly less energy and exhibit brittle behavior, while cracks propagating across layers (intralayer) demand roughly 10 times more energy and display ductile, elastic–plastic behavior. Microscopy reveals that porosity and weak weld lines between layers contribute to brittle fracture, despite ductile features at the microscale. In specimens with oblique orientations, cracks tend to kink toward weaker interlayer paths. The research highlights that optimizing lamina orientation, inspired by natural materials like wood and bone, can improve the toughness and reliability of additively manufactured components

Infrared thermography was used by Seppala et al. [85] to monitor temperature during ME printing of ABS, with a focus on interlayer bonding. It was found that the extruded material cools rapidly, at a rate of approximately 100 °C/s, which means it remains above the glass transition temperature for only one second, thereby limiting interlayer bond strength. Calibrated infrared imaging revealed that only the top layer briefly reaches 155 °C, while the underlying layers remain too cool to enable strong bonding. These findings help explain common interlayer failures and suggest that infrared thermography can be utilized to optimize printing conditions for the production of stronger and more reliable parts.

A burst detection was conducted with CiteSpace to identify the top 20 keyword with the strongest citation burst. The result is inserted as Figure 5. From a material perspective, ABS bursted between 2016 and 2019, while PLA was cited more recently.

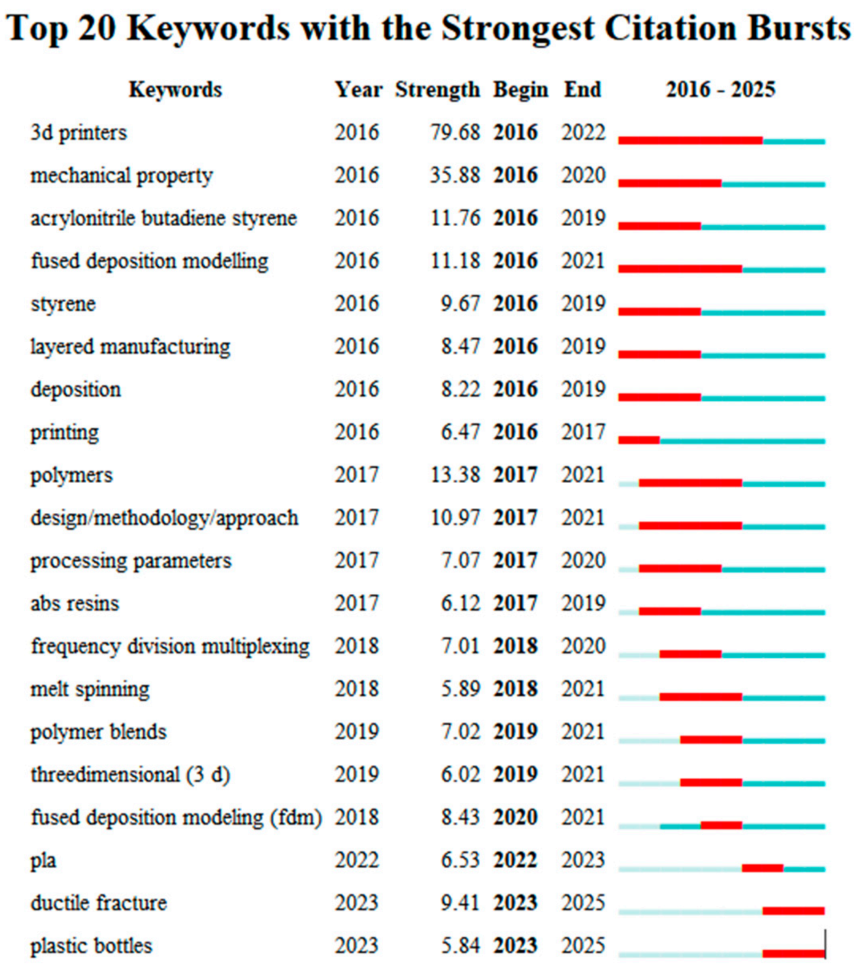

Figure 5. Keyword burst result. The red bar is for highlighting the burst duration, the turquoise bar to represent the years of significant occurrence of the keyword, and the light-blue bar to indicate the years of no significant occurrence of the keyword.

4. Discussion

This systematic review highlights the significant research and ongoing limitations in additive manufacturing, particularly focusing on ME and material extrusion processes, and examines how various process parameters and material factors influence the mechanical properties of the resulting parts. Over the last 10 years, an increasing number of articles have been published on the topic of how printing parameters, material structure, and post-processing techniques influence the mechanical properties and overall performance of 3D-printed parts.

From a manufacturing technology point of view, the following main research has been explored:

Novel extruder designs and hybrid material systems further improve the properties of printable composites [42], despite issues such as void formation [47,59] and fiber–matrix debonding [67]. These microstructural flaws are linked to process parameters such as printing speed, temperature, and layer thickness, which directly affect the interlayer bonding quality and dimensional accuracy [50]. The review highlighted the importance of optimizing thermal conditions during printing, as rapid cooling rates can cause insufficient interdiffusion between layers, severely limiting mechanical strength, especially in amorphous polymers [71,85]. Studies on thermal in situ and post processing reveal promising improvements in crystallinity and mechanical behavior [71]. Innovations in process monitoring and control, including real-time defect detection via computer vision and the application of near-infrared laser preheating, show great potential in improving print reliability and mechanical performance [71]. However, achieving consistent quality and scalability remains a challenge, particularly in the context of commercial and industrial applications where productivity and repeatability are paramount. Tlegenov et al. [72] introduced a vibration-based nozzle-clogging detection technique that enables low-cost, real-time monitoring of a common defect source in ME printing, potentially improving print reliability and reducing downtime. Complementing these findings, Reich et al. [78] explored fused granular fabrication (FGF), revealing trade-offs between high deposition rates and mechanical properties, suggesting its use as a technique complementary to traditional ME for applications where fine resolution and compressive strength are critical. Additionally, Bodaghi et al. [79] demonstrated that 4D printing strategies can program self-transforming behaviors into printed parts by manipulating residual stresses through printing parameters, opening new frontiers for adaptive and biomedical applications.

Emerging technologies in manufacturing are enhancing process control and print reliability in material extrusion additive manufacturing. Real-time defect detection methods, such as computer vision systems and vibration-based nozzle-clogging monitoring introduced by Tlegenov et al. [72], enable low-cost, continuous quality assurance, reducing downtime and improving consistency. Near-infrared laser preheating has shown promise in optimizing thermal conditions to strengthen interlayer bonding [71]. Additionally, fused granular fabrication (FGF), as explored by Reich et al. [78], offers an approach complementary to traditional ME by enabling higher deposition rates, which may suit specific applications requiring compressive strength over fine resolution. Furthermore, 4D printing techniques demonstrated by Bodaghi et al. [79] introduce controlled residual stresses to program self-transforming behaviors into printed parts, offering a pathway to many abilities, like adaptive structures and biomedical devices.

From a material science perspective, the development of predictive printability models [69] and the evaluation of micro- and mesostructural factors provide critical insights into the design of next-generation printable composites [74,75]. Key findings from the literature show that the integration of continuous and short fiber reinforcements, such as carbon, glass, aramid, and natural fibers (flax), markedly enhances tensile strength, stiffness, and flexural performance compared to pure polymer matrices like PLA and ABS [52,67,68,80]. The ability to influence the mesostructure, chemical composition, and filler orientation offers routes to mitigate anisotropy and enhance part robustness [64,69]. Moreover, the sustainability aspect is gaining attention with biodegradable materials, recycled polymers, and natural fiber reinforcements, which align with broader environmental goals without compromising mechanical integrity [52–54]. Studies by Dou et al. [75], Iragi et al. [76], and Calignano et al. [77] emphasize how printing parameters such as layer height, extrusion width, build orientation, and infill percentage directly influence the mechanical performance and anisotropic nature of fiber-reinforced prints. Mechanical characterization work by Davis et al. [80] and Hart and Wetzel [81] further underscores the dominant role of printing temperature and layer orientation in governing interlayer weld strength and fracture behavior in ABS, highlighting the ongoing need to optimize process parameters to overcome inherent anisotropy and brittleness.

In material science, emerging approaches focus on enhancing composite design and sustainability in 3D printing. Predictive printability models [69] assist in anticipating material behavior and optimizing print parameters for improved outcomes. The integration of continuous and short fiber reinforcements—including carbon, glass, aramid, and natural fibers such as flax—significantly elevates tensile strength, stiffness, and flexural performance beyond those of pure polymer matrices [52,67,68,80]. Methods focused on mesostructure, chemical composition, and filler orientation offer solutions to mitigate anisotropy and bolster part robustness [64,69]. Sustainability-driven methods can use biodegradable and recycled polymers combined with natural fiber reinforcements, aligning mechanical performance with environmental considerations [52–54]. These emerging technologies collectively offer printable composite capabilities and align additive manufacturing to be more ecologically friendly.

In conclusion, while ME and related extrusion-based additive manufacturing technologies have matured significantly, ongoing research must continue to address the intrinsic limitations imposed by material behavior, interlayer adhesion, and microstructural defects. Future work should focus on integrating advanced process control strategies, exploring hybrid and multi-material systems, and developing comprehensive models that link process parameters with mechanical outcomes. Such efforts will be essential for expanding the applicability of additive manufacturing to high-performance engineering components, enabling not only improved mechanical properties but also greater sustainability and cost-effectiveness in production.

Several reviewed articles incorporated physical modeling to optimize ME processes and predict part performance. Bodaghi et al. [82] used finite element analysis (FEA) with constitutive modeling, based on non-linear Green–Lagrange strains and solved via the Newton–Raphson scheme, to simulate shape-memory polymer behavior in 4D printing. Duty et al. [73] developed a “Printability Model” with bounding equations, including a nozzle flow criterion from the Hagen–Poiseuille equation adapted for non-Newtonian fluids, to assess extrusion feasibility. Ravi et al. [71] applied transient heat transfer FEA in COMSOL to model near-infrared laser preheating, predicting temperature profiles that improve interlayer bonding. Kabir et al. [66] summarized predictive models such as FEA, Volume Averaging Stiffness, Rule of Mixing, and Hashin’s damage criteria to evaluate and enhance mechanical properties of continuous fiber-reinforced ME composites.

And now at the end, Table 1 summarizes the major findings of the review papers with references. The fourth column of the table also indicates which research questions were answered by the articles.

Table 1. Summary table of the various articles.

Feature	Relationships	References	Research Questions
Printing Process Parameters	Higher nozzle and bed temps improve interlayer bonding and strength Layer height significantly affects mechanical strength Printing speed influences extrusion quality and dimensional accuracy	Yin et al. [50] Spoerk et al. [74] Geng et al. [49]	RQ1
Void Formation	Voids reduce tensile/flexural strength significantly Minimizing void volume improves mechanical properties	He et al. [47] Aliheidari et al. [59]	RQ3
Crystalline Structure	Increased crystallinity enhances stiffness, strength, and thermal stability Annealing post print improves crystallinity but may cause thermal damage	Wittbrodt et al. [76]	RQ2/RQ3
Fiber Reinforcement	Continuous fibers improve tensile strength and stiffness significantly Fiber type and matrix bonding are critical for performance	Duigou et al. [52] Wang et al. [45]	RQ3
Thermal Effects	Cooling rates affect interlayer adhesion, and rapid cooling limits bonding Preheating layers improves bonding and reduces brittleness 4D printing strategies can program self-transforming behaviors into printed parts	Seppala et al. [85] Ravi et al. [71] Bodaghi etal. [82]	RQ1
Build Orientation and Layup	Flat orientation increases strength and stiffness Unidirectional layups yield higher strength but more brittleness Alternating layups improve isotropy	Chacón et al. [68] Kiendl et al. [69]	RQ1
Surface Treatments	Surface prep of fibers enhances bonding and mechanical strength	Heidari-Rarani et al. [42]	RQ2
Material Recycling	Recycled materials show reduced mechanical properties but maintain some usability	Anderson et al. [53]	RQ3
Manufacturing Monitoring	Real-time defect detection improves print quality Thermal monitoring guides process adjustments Real-time vibration-based nozzle-clogging detection technique	Jin et al. [70] eppala et al. [85] Tlegenov et al. [72]	RQ2
Weld Strength/ Interlayer Bond	Printing temperature critically affects weld strength Propagating interlayer cracks requires 10 less energy than propagating intralayer cracks	Davis et al. [83] Hart and Wetzel [84]	RQ1
Printability Modeling	The “Printability Model” predicts whether materials are printable based on nozzle flow, fiber clogging, geometry creation, and stability—useful for screening material feasibility	Duty et al. [73]	RQ3

Predictive models based on process parameters and material properties should be extensively utilized in future research to increase the reliability of ME systems across a wide variety of materials. The development of closed-loop control systems based on sensor data represents a promising direction for improving part quality and reducing material waste. Additionally, integrating micro- and mesostructural research into the manufacturing process should be prioritized to mitigate anisotropy and void formation, two key factors that significantly reduce the mechanical performance of printed parts.

This study has several limitations. First, the selected query and applied filters substantially influenced the dataset, potentially excluding relevant articles that address the research questions. Medical applications of ME were deliberately excluded from this review, despite being a key area where additive manufacturing offers significant advantages through the rapid production of customized, patient-specific parts. Secondly, the review is heavily focused on mechanical properties, which may overlook other critical performance metrics such as chemical resistance, electrical behavior, and fatigue performance. Articles involving dynamic mechanical analysis are notably under-represented. Third, although additive manufacturing encompasses a broad range of materials and technologies, this study is limited to extrusion-based methods and does not address other techniques, such as SLA, SLS, or DED.

Author Contributions: Conceptualization, A.D. and S.B.; methodology, Z.B.; software, A.D. and Z.B.; investigation, A.D.; data curation, A.D.; writing—original draft preparation, A.D.; writing—review and editing, A.D., Z.B. and S.B.; visualization, A.D. All authors have read and agreed to the published version of the manuscript.

Funding: This research received no external funding.

Data Availability Statement: The original contributions presented in this study are included in the article; further inquiries can be directed to the corresponding author.

Acknowledgments: Supported by the University of Debrecen.

Conflicts of Interest: The authors declare no conflicts of interest.

Abbreviations

The following abbreviations are used in this manuscript:

BAAM	Big Area Additive Manufacturing
CF	Carbon Fiber
DED	Directed Energy Deposition
FDM	Fused Deposition Modeling
FFF	Fused Filament Fabrication
GF	Glass Fiber
ME	Material Extrusion
MEMS	Micro-ElectroMechanical System
SMP	Shape Memory Polymer
xGnP	Exfoliated Graphite nanoplatelets

References

1. Wohlers, T.; Gornet, T.; Mostow, N.; Campbell, I.; Diegel, O.; Kowen, J.; Huff, R.; Stucker, B.; Fidan, I.; Doukas, A.; et al. History of Additive Manufacturing. *SSRN Electron. J.* **2023**. [CrossRef]
2. Divakaran, N.; Das, J.P.; Kumar, A.; Mohanty, S.; Ramadoss, A.; Nayak, S.K. Comprehensive review on various additive manufacturing techniques and its implementation in electronic devices. *J. Manuf. Syst.* **2022**, *62*, 477–502. [CrossRef]
3. Godec, D.; Gonzalez-Gutierrez, J.; Nordin, A.; Pei, E.; Ureña, J. *A Guide to Additive Manufacturing*; Springer Nature: Berlin/Heidelberg, Germany, 2022; pp. 9–10, 28–30, 35–37.

4. Praveena, B.A.; Lokesh, N.; Santhosh, N.; Praveena, B.L.; Vignesh, R. A comprehensive review of emerging additive manufacturing (3D printing technology): Methods, materials, applications, challenges, trends and future potential. *Mater. Today: Proc.* **2022**, *52*, 1309–1313. [CrossRef]
5. Guessasma, S.; Zhang, W.; Zhu, J.; Belhabib, S.; Nouri, H. Challenges of additive manufacturing technologies from an optimisation perspective. *Int. J. Simul. Multidiscip. Des. Optim.* **2015**, *6*, A9. [CrossRef]
6. Loh, G.H.; Pei, E.; Gonzalez-Gutierrez, J.; Monzón, M. An Overview of Material Extrusion Troubleshooting. *Appl. Sci.* **2020**, *10*, 4776. [CrossRef]
7. Abdulhameed, O.; Al-Ahmari, A.; Ameen, W.; Mian, S.H. Additive manufacturing Challenges, trends, and applications. *Adv. Mech. Eng.* **2019**, *11*, 1–27. [CrossRef]
8. Tofail, S.; Koumoulos, E.; Bandyopadhyay, A.; Bose, S.; O'Donoghue, L.; Charitidis, C.A. Additive manufacturing: Scientific and technological challenges, market uptake and opportunities. *Mater. Today* **2017**, *21*, 22–37. [CrossRef]
9. Srivastava, M.; Rathee, S.; Patel, V.; Kumar, A.; Koppad, P.G. A review of various materials for additive manufacturing: Recent trends and processing issues. *J. Mater. Res. Technol.* **2022**, *21*, 2612–2641. [CrossRef]
10. Bourell, D.; Kruth, J.P.; Leu, M.; Levy, G.; Rosen, D.; Beese, A.M.; Clare, A. Materials for additive manufacturing. *CIRP Ann.* **2017**, *66*, 659–681. [CrossRef]
11. Wypych, G. *Handbook of Polymers*, 3rd ed.; ChemTec Publishing: Toronto, ON, Canada, 2022.
12. Rudin, A.; Choi, P. Chapter 1—Introductory Concepts and Definitions. In *The Elements of Polymer Science & Engineering*, 3rd ed.; Rudin, A., Choi, P., Eds.; Academic Press: Boston, MA, USA, 2013; pp. 1–62.
13. Chanda, S.K.R.M. *Plastics Technology Handbook*, 4th ed.; CRC Press: Boca Raton, FL, USA, 2006.
14. Peters, E. Plastics: Thermoplastics, Thermosets, and Elastomers. In *Handbook of Materials Selection*; Wiley: Hoboken, NJ, USA, 2007; pp. 335–355.
15. Pascault, J.P.; Williams, R.J.J. Chapter 1—Overview of thermosets: Present and future. In *Thermosets*, 2nd ed.; Guo, Q., Ed.; Elsevier: Amsterdam, The Netherlands, 2018; pp. 3–34.
16. Shanmugam, V.; Babu, K.; Kannan, G.; Mensah, R.A.; Samantaray, S.K.; Das, O. The thermal properties of FDM printed polymeric materials: A review. *Polym. Degrad. Stab.* **2024**, *228*, 110902. [CrossRef]
17. Swetham, T.; Reddy, K.M.M.; Huggi, A.; Kumar, M.N. A Critical Review on of 3D Printing Materials and Details of Materials used in FDM. *Int. J. Sci. Res. Sci. Eng. Technol.* **2017**, *3*, 353–361.
18. Belaid, H.; Nagarajan, S.; Teyssier, C.; Barou, C.; Barés, J.; Balme, S.; Garay, H.; Huon, V.; Cornu, D.; Cavaillès, V.; et al. Development of new biocompatible 3D printed graphene oxide-based scaffolds. *Mater. Sci. Eng. C Mater. Biol. Appl.* **2020**, *110*, 110595. [CrossRef]
19. Li, N.; Li, Y.; Liu, S. Rapid prototyping of continuous carbon fiber reinforced polylactic acid composites by 3D printing. *J. Mech. Work. Technol.* **2016**, *238*, 218–225. [CrossRef]
20. Tymrak, B.M.; Kreiger, M.; Pearce, J.M. Mechanical properties of components fabricated with open-source 3-D printers under realistic environmental conditions. *Mater. Des.* **2014**, *58*, 242–246. [CrossRef]
21. Khan, S.; Joshi, K.; Deshmukh, S. A comprehensive review on effect of printing parameters on mechanical properties of FDM printed parts. *Mater. Today Proc.* **2022**, *50*, 2119–2127. [CrossRef]
22. Utracki, L.A. History of commercial polymer alloys and blends (from a perspective of the patent literature). *Polym. Eng. Sci.* **1995**, *35*, 2–17. [CrossRef]
23. Rodríguez, J.F.; Thomas, J.P.; Renaud, J.E. Mechanical behavior of acrylonitrile butadiene styrene (ABS) fused deposition materials. Experimental investigation. *Rapid Prototyp. J.* **2001**, *7*, 148–158. [CrossRef]
24. Ning, F.; Cong, W.; Qiu, J.; Wei, J.; Wang, S. Additive manufacturing of carbon fiber reinforced thermoplastic composites using fused deposition modeling. *Compos. Part B Eng.* **2015**, *80*, 369–378. [CrossRef]
25. Shakiba, M.; Ghomi, E.R.; Khosravi, F.; Jouybar, S.; Bigham, A.; Zare, M.; Abdouss, M.; Moaref, R.; Ramakrishna, S. PA—A material introduction and overview for biomedical applications. *Polym. Adv. Technol.* **2021**, *32*, 3368–3383. [CrossRef]
26. Banjo, A.D.; Agrawal, V.; Auad, M.L.; Celestine, A.-D.N. Moisture-induced changes in the mechanical behavior of 3D printed polymers. *Compos. Part C Open Access* **2022**, *7*, 100243. [CrossRef]
27. Batista-Canino, R.M.; Santana-Hernandez, L.; Medina-Brito, P. A scientometric analysis on entrepreneurial intention literature: Delving deeper into local citation. *Heliyon* **2023**, *9*, e13046. [CrossRef] [PubMed]
28. Boyack, K.W.; Klavans, R. Co-citation analysis, bibliographic coupling, and direct citation: Which citation approach represents the research front most accurately? *J. Am. Soc. Inf. Sci. Technol.* **2010**, *61*, 2389–2404. [CrossRef]
29. Donthu, N.; Kumar, S.; Mukherjee, D.; Pandey, N.; Lim, W.M. How to conduct a bibliometric analysis: An overview and guidelines. *J. Bus. Res.* **2021**, *133*, 285–296. [CrossRef]
30. Yan, E.; Ding, Y. Scholarly network similarities: How bibliographic coupling networks, citation networks, cocitation networks, topical networks, coauthorship networks, and coword networks relate to each other. *J. Am. Soc. Inf. Sci. Technol.* **2012**, *63*, 1313–1326. [CrossRef]

31. Arruda, H.; Silva, E.R.; Lessa, M.; Proenca, D., Jr.; Bartholo, R. VOSviewer and Bibliometrix. *J. Med. Libr. Assoc.* **2022**, *110*, 392–395. [CrossRef]
32. van Eck, N.J.; Waltman, L. Citation-based clustering of publications using CitNetExplorer and VOSviewer. *Scientometrics* **2017**, *111*, 1053–1070. [CrossRef]
33. Kleinberg, J. Bursty and Hierarchical Structure in Streams. *Data Min. Knowl. Discov.* **2003**, *7*, 373–397. [CrossRef]
34. Amjad, T.; Shahid, N.; Daud, A.; Khatoon, A. Citation burst prediction in a bibliometric network. *Scientometrics* **2022**, *127*, 2773–2790. [CrossRef]
35. Chen, C. CiteSpace II: Detecting and visualizing emerging trends and transient patterns in scientific literature. *J. Am. Soc. Inf. Sci. Technol.* **2005**, *57*, 359–377. [CrossRef]
36. Chen, C. *CiteSpace: A Practical Guide for Mapping Scientific Literature*; Nova Science Publishers: Hauppauge, NY, USA, 2016.
37. Radhakrishnan, S.; Erbis, S.; Isaacs, J.A.; Kamarthi, S. Novel keyword co-occurrence network-based methods to foster systematic reviews of scientific literature. *PLoS ONE* **2017**, *12*, e0172778. [CrossRef]
38. Klarin, A. How to conduct a bibliometric content analysis: Guidelines and contributions of content co-occurrence or co-word literature reviews. *Int. J. Consum. Stud.* **2024**, *48*, e13031. [CrossRef]
39. Baas, J.; Schotten, M.; Plume, A.; Côté, G.; Karimi, R. Scopus as a curated, high-quality bibliometric data source for academic research in quantitative science studies. *Quant. Sci. Stud.* **2020**, *1*, 377–386. [CrossRef]
40. Thelwall, M.; Sud, P. Scopus 1900–2020: Growth in articles, abstracts, countries, fields, and journals. *Quant. Sci. Stud.* **2022**, *3*, 37–50. [CrossRef]
41. Pranckutė, R. Web of Science (WoS) and Scopus: The Titans of Bibliographic Information in Today's Academic World. *Publications* **2021**, *9*, 12. [CrossRef]
42. Heidari-Rarani, M.; Rafiee-Afarani, M.; Zahedi, A.M. Mechanical characterization of FDM 3D printing of continuous carbon fiber reinforced PLA composites. *Compos. Part B Eng.* **2019**, *175*, 107147. [CrossRef]
43. Senatov, F.S.; Niaza, K.V.; Zadorozhnyy, M.Y.; Maksimkin, A.V.; Kaloshkin, S.D.; Estrin, Y.Z. Mechanical properties and shape memory effect of 3D-printed PLA-based porous scaffolds. *J. Mech. Behav. Biomed. Mater.* **2016**, *57*, 139–148. [CrossRef] [PubMed]
44. Dul, S.; Fambri, L.; Pegoretti, A. Fused deposition modelling with ABS–graphene nanocomposites. *Compos. Part A Appl. Sci. Manuf.* **2016**, *85*, 181–191. [CrossRef]
45. Wang, P.; Zou, B.; Ding, S.; Huang, C.; Shi, Z.; Ma, Y.; Yao, P. Preparation of short CF/GF reinforced PEEK composite filaments and their comprehensive properties evaluation for FDM-3D printing. *Compos. Part B Eng.* **2020**, *198*, 108175. [CrossRef]
46. Liu, H.; Wang, F.; Wu, W.; Dong, X.; Sang, L. 4D printing of mechanically robust PLA/TPU/Fe3O4 magneto-responsive shape memory polymers for smart structures. *Compos. Part B Eng.* **2023**, *248*, 110382. [CrossRef]
47. He, Q.; Wang, H.; Fu, K.; Ye, L. 3D printed continuous CF/PA6 composites: Effect of microscopic voids on mechanical performance. *Compos. Sci. Technol.* **2020**, *191*, 108077. [CrossRef]
48. Duty, C.E.; Kunc, V.; Compton, B.; Post, B.; Erdman, D.; Smith, R.; Lind, R.; Lloyd, P.; Love, L. Structure and mechanical behavior of Big Area Additive Manufacturing (BAAM) materials. *Rapid Prototyp. J.* **2017**, *23*, 181–189. [CrossRef]
49. Geng, P.; Zhao, J.; Wu, W.; Ye, W.; Wang, Y.; Wang, S.; Zhang, S. Effects of extrusion speed and printing speed on the 3D printing stability of extruded PEEK filament. *J. Manuf. Process.* **2019**, *37*, 266–273. [CrossRef]
50. Yin, J.; Lu, C.; Fu, J.; Huang, Y.; Zheng, Y. Interfacial bonding during multi-material fused deposition modeling (FDM) process due to inter-molecular diffusion. *Mater. Des.* **2018**, *150*, 104–112. [CrossRef]
51. Le Duigou, A.; Barbé, A.; Guillou, E.; Castro, M. 3D printing of continuous flax fibre reinforced biocomposites for structural applications. *Mater. Des.* **2019**, *180*, 107884. [CrossRef]
52. van Eck, N.J.; Waltman, L. How to normalize cooccurrence data? An analysis of some well-known similarity measures. *J. Am. Soc. Inf. Sci. Technol.* **2009**, *60*, 1635–1651. [CrossRef]
53. Anderson, I. Mechanical Properties of Specimens 3D Printed with Virgin and Recycled Polylactic Acid. *3D Print. Addit. Manuf.* **2017**, *4*, 110–115. [CrossRef]
54. Sanchez, F.A.C.; Boudaoud, H.; Hoppe, S.; Camargo, M. Polymer recycling in an open-source additive manufacturing context: Mechanical issues. *Addit. Manuf.* **2017**, *17*, 87–105. [CrossRef]
55. Hikmat, M.; Rostam, S.; Ahmed, Y.M. Investigation of tensile property-based Taguchi method of PLA parts fabricated by FDM 3D printing technology. *Results Eng.* **2021**, *11*, 100264. [CrossRef]
56. Ivey, M.; Melenka, G.W.; Carey, J.P.; Ayranci, C. Characterizing short-fiber-reinforced composites produced using additive manufacturing. *Adv. Manuf. Polym. Compos. Sci.* **2017**, *3*, 81–91. [CrossRef]
57. Gkartzou, E.; Koumoulos, E.P.; Charitidis, C.A. Production and 3D printing processing of bio-based thermoplastic filament. *Manuf. Rev.* **2017**, *4*, 1. [CrossRef]

58. Abbott, A.C.; Tandon, G.P.; Bradford, R.L.; Koerner, H.; Baur, J.W. Process-structure-property effects on ABS bond strength in fused filament fabrication. *Addit. Manuf.* **2018**, *19*, 29–38. [CrossRef]
59. Aliheidari, N.; Christ, J.; Tripuraneni, R.; Nadimpalli, S.; Ameli, A. Interlayer adhesion and fracture resistance of polymers printed through melt extrusion additive manufacturing process. *Mater. Des.* **2018**, *156*, 351–361. [CrossRef]
60. Hu, Q.; Duan, Y.; Zhang, H.; Liu, D.; Yan, B.; Peng, F. Manufacturing and 3D printing of continuous carbon fiber prepreg filament. *J. Mater. Sci.* **2017**, *53*, 1887–1898. [CrossRef]
61. Bettini, P.; Alitta, G.; Sala, G.; Di Landro, L. Fused Deposition Technique for Continuous Fiber Reinforced Thermoplastic. *J. Mater. Eng. Perform.* **2016**, *26*, 843–848. [CrossRef]
62. Alaimo, G.; Marconi, S.; Costato, L.; Auricchio, F. Influence of meso-structure and chemical composition on FDM 3D-printed parts. *Compos. Part B Eng.* **2017**, *113*, 371–380. [CrossRef]
63. Hmeidat, N.S.; Kemp, J.W.; Compton, B.G. High-strength epoxy nanocomposites for 3D printing. *Compos. Sci. Technol.* **2018**, *160*, 9–20. [CrossRef]
64. Gao, X.; Qi, S.; Kuang, X.; Su, Y.; Li, J.; Wang, D. Fused filament fabrication of polymer materials: A review of interlayer bond. *Addit. Manuf.* **2021**, *37*, 101658. [CrossRef]
65. Wang, P.; Zou, B.; Xiao, H.; Ding, S.; Huang, C. Effects of printing parameters of fused deposition modeling on mechanical properties, surface quality, and microstructure of PEEK. *J. Mater. Process. Technol.* **2019**, *271*, 62–74. [CrossRef]
66. Kabir, S.M.F.; Mathur, K.; Seyam, A.-F.M. A critical review on 3D printed continuous fiber-reinforced composites: History, mechanism, materials and properties. *Compos. Struct.* **2020**, *232*, 111476. [CrossRef]
67. Wickramasinghe, S.; Do, T.; Tran, P. FDM-Based 3D Printing of Polymer and Associated Composite: A Review on Mechanical Properties, Defects and Treatments. *Polymers* **2020**, *12*, 1529. [CrossRef]
68. Chacón, J.M.; Caminero, M.A.; Núñez, P.J.; García-Plaza, E.; García-Moreno, I.; Reverte, J.M. Additive manufacturing of continuous fibre reinforced thermoplastic composites using fused deposition modelling: Effect of process parameters on mechanical properties. *Compos. Sci. Technol.* **2019**, *181*, 107688. [CrossRef]
69. Kiendl, J.; Gao, C. Controlling toughness and strength of FDM 3D-printed PLA components through the raster layup. *Compos. Part B Eng.* **2020**, *180*, 11–15. [CrossRef]
70. Jin, Z.; Zhang, Z.; Gu, G.X. Autonomous in-situ correction of fused deposition modeling printers using computer vision and deep learning. *Manuf. Lett.* **2019**, *22*, 11–15. [CrossRef]
71. Ravi, A.K.; Deshpande, A.; Hsu, K.H. An in-process laser localized pre-deposition heating approach to inter-layer bond strengthening in extrusion based polymer additive manufacturing. *J. Manuf. Process.* **2016**, *24*, 179–185. [CrossRef]
72. Tlegenov, Y.; Hong, G.S.; Lu, W.F. Nozzle condition monitoring in 3D printing. *Robot. Comput. Manuf.* **2018**, *54*, 45–55. [CrossRef]
73. Duty, C.; Ajinjeru, C.; Kishore, V.; Compton, B.; Hmeidat, N.; Chen, X.; Liu, P.; Hassen, A.A.; Lindahl, J.; Kunc, V. What makes a material printable? A viscoelastic model for extrusion-based 3D printing of polymers. *J. Manuf. Process.* **2018**, *35*, 526–537. [CrossRef]
74. Spoerk, M.; Arbeiter, F.; Cajner, H.; Sapkota, J.; Holzer, C. Parametric optimization of intra- and inter-layer strengths in parts produced by extrusion-based additive manufacturing of poly(lactic acid). *J. Appl. Polym. Sci.* **2017**, *134*, 45401. [CrossRef]
75. Tanikella, N.G.; Wittbrodt, B.; Pearce, J.M. Tensile strength of commercial polymer materials for fused filament fabrication 3D printing. *Addit. Manuf.* **2017**, *15*, 40–47. [CrossRef]
76. Wittbrodt, B.; Pearce, J.M. The effects of PLA color on material properties of 3-D printed components. *Addit. Manuf.* **2015**, *8*, 110–116. [CrossRef]
77. Wach, R.A.; Wolszczak, P.; Adamus-Wlodarczyk, A. Enhancement of Mechanical Properties of FDM-PLA Parts via Thermal Annealing. *Macromol. Mater. Eng.* **2018**, *303*, 1800169. [CrossRef]
78. Dou, H.; Cheng, Y.; Ye, W.; Zhang, D.; Li, J.; Miao, Z.; Rudykh, S. Effect of Process Parameters on Tensile Mechanical Properties of 3D Printing Continuous Carbon Fiber-Reinforced PLA Composites. *Materials* **2020**, *13*, 3850. [CrossRef] [PubMed]
79. Iragi, M.; Pascual-González, C.; Esnaola, A.; Lopes, C.S.; Aretxabaleta, L. Ply and interlaminar behaviours of 3D printed continuous carbon fibre-reinforced thermoplastic laminates; effects of processing conditions and microstructure. *Addit. Manuf.* **2019**, *30*, 100884. [CrossRef]
80. Calignano, F.; Lorusso, M.; Roppolo, I.; Minetola, P. Investigation of the Mechanical Properties of a Carbon Fibre-Reinforced PA Filament for 3D Printing. *Machines* **2020**, *8*, 52. [CrossRef]
81. Reich, M.J.; Woern, A.L.; Tanikella, N.G.; Pearce, J.M. Mechanical Properties and Applications of Recycled Polycarbonate Particle Material Extrusion-Based Additive Manufacturing. *Materials* **2019**, *12*, 1642. [CrossRef]
82. Bodaghi, M.; Damanpack, A.R.; Liao, W.H. Adaptive metamaterials by functionally graded 4D printing. *Mater. Des.* **2017**, *135*, 26–36. [CrossRef]

83. Davis, C.S.; Hillgartner, K.E.; Han, S.H.; Seppala, J.E. Mechanical strength of welding zones produced by material extrusion additive manufacturing. *Addit. Manuf.* **2017**, *16*, 162–166. [CrossRef] [PubMed]
84. Hart, K.R.; Wetzel, E.D. Fracture behavior of additively manufactured acrylonitrile butadiene styrene (ABS) materials. *Eng. Fract. Mech.* **2017**, *177*, 1–13. [CrossRef]
85. Seppala, J.E.; Migler, K.D. Infrared thermography of welding zones produced by polymer extrusion additive manufacturing. *Addit. Manuf.* **2016**, *12*, 71–76. [CrossRef]